A New Frequency Domain Symmetrical Condensed TLM Node

Pierre Berini, *Student Member, IEEE,* and Ke Wu, *Senior Member, IEEE*

***Abstract*—This paper reports the development of a new symmetrical condensed TLM node derived directly in the frequency domain. The new node can accommodate a graded mesh and can model lossy anisotropic media described by a static conductivity tensor along with complex permittivity and complex permeability tensors. The frequency domain TLM method is used to generate modal dispersion curves for mWave and mmWave guiding structures. The results compare the new node to existing time domain symmetrical condensed nodes.**

I. Introduction

The TLM technique has recently been applied in the frequency domain [1], [2], where the major advantages of TLM simulation have been conserved; namely, the ease with which electromagnetic fields in inhomogeneous and complex media can be simulated. Time domain nodes, such as the symmetrical condensed node [3], [4], [5] or the hybrid symmetrical condensed node [6], are inherently ill-suited to frequency domain analysis as both nodes use open or short circuited stubs to model the characteristics of the medium where propagation takes place. These stubs add numerical dispersion when the permittivity or permeability of the medium increases. A lossless frequency domain node was originally proposed by Johns [2] where the phase constant of the link lines are varied to account for mesh grading and the local properties of the medium. The characteristic impedance of the link lines are the same and take on the value of the intrinsic impedance occupying the space inside the TLM cell. If the medium to be modelled is inhomogeneous, then scattering may occur at the connection plane between two link lines.

This paper reports the development of a generalized symmetrical condensed TLM node derived directly in the frequency domain. This new 12×12 node is stubless and models local variations in mesh size, conductivity, complex permittivity, and complex permeability by varying the complex characteristic impedance and propagation constant of the link lines. Anisotropic conductivities, permittivities, and permeabilities can be modelled by the node if the tensors involved are diagonal. The frequency domain node is suitable for use with the steady-state TLM Method [2] or the FD-TLM method [7], [8].

Manuscript received January 28, 1994.
The authors are with the Département de génie électrique et informatique, École Polytechnique de Montréal, POLY-GRAMES, Station Centre Ville, Montréal, Québec, H3C 3A7, Canada.
IEEE Log Number 9402179.

II. Formulation

Maxwell's curl equations in the frequency domain are written for lossy anisotropic media:

$$\nabla \times \mathbf{E} = -([\sigma_m] + j\omega[\mu'])\mathbf{H} \tag{1}$$

$$\nabla \times \mathbf{H} = ([\sigma_e] + j\omega[\epsilon'])\mathbf{E} \tag{2}$$

where $[\sigma_m]$, $[\sigma_e]$, $[\mu']$ and $[\epsilon']$ are diagonal tensors sharing common principal axes. The components of the conductivity tensors are defined as $\sigma_{m,i} = \omega\mu_i''$ and $\sigma_{e,i} = \sigma_{\mathrm{se},i} + \omega\epsilon_i''$ where $i \in \{x, y, z\}$. $\sigma_{\mathrm{se},i}$ is the static electrical conductivity along the i axis.

A. Lossy Anisotropic Media

The frequency domain symmetrical condensed node shares the numbering scheme and geometry of the stubless node given in [3]. In a manner similar to time domain TLM theory [3], [9], an analogy is drawn between Maxwell's frequency domain curl equations, written in component form, and the equations governing the propagation of complex voltage waves on the transmission line network. This analogy yields six equivalence relations that relate the complex characteristic impedance and propagation constant of the link lines to the local dimensions of the mesh and properties of the medium to be modelled. From these TLM equivalence relations, we obtain the characteristic impedance and propagation constants of the link lines:

$$\gamma_{pq} = \frac{1}{2}\sqrt{(\sigma_{e,q} + j\omega\epsilon_q')(\sigma_{m,r} + j\omega\mu_r')} \tag{3}$$

$$Z_{pq} = \frac{\Delta_q}{\Delta_r}\sqrt{\frac{(\sigma_{m,r} + j\omega\mu_r')}{(\sigma_{e,q} + j\omega\epsilon_q')}} \tag{4}$$

where $p, q, r \in \{x, y, z\}$, $p \neq q \neq r$ and six different pairs pq are generated. For example, if $p = z$ and $q = x$ then $\gamma_{pq} = \gamma_{zx}$ refers to the propagation constant of the lines carrying V_9 and V_2, polarized along x and propagating along z. The characteristic impedance of a link line may vary from node to node if the medium to be modelled is inhomogeneous or if the mesh grading varies across the structure. The connection of the link lines at the center of the node is described by the voltage scattering matrix S_v in (5).

$$\mathbf{V}^{\mathrm{ref}} = [S_v]\mathbf{V}^{\mathrm{inc}} \tag{5}$$

where

$$\mathbf{V}^{\mathrm{inc,ref}} = [\mathbf{V}_1^{\mathrm{inc,ref}}, \ldots, V_{12}^{\mathrm{inc,ref}}]^t$$

and the matrix S_v shown at the bottom of the next page.

The elements of the matrix S_v are determined by imposing the conservation of charge, the conservation of magnetic flux, the continuity of the electric field, and the continuity of the magnetic field to the node [10]:

$$a_{pq} = \frac{Z_{qp}}{z_{qp} + Z_{rp}} - \frac{Z_{rp}}{Z_{rp} + Z_{pr}} = b_{pr} - d_{pq} \tag{6}$$

$$c_{pq} = \frac{Z_{rp}}{Z_{rp} + Z_{pr}} - \frac{Z_{rp}}{Z_{rp} + Z_{qp}} = d_{pq} - b_{pq} \tag{7}$$

$$b_{pq} = \frac{Z_{rp}}{Z_{rp} + Z_{qp}} \tag{8}$$

$$d_{pq} = \frac{Z_{rp}}{Z_{rp} + Z_{pr}} \tag{9}$$

where $p, q, r \in \{x, y, z\}, p \neq q \neq r$. For the special case of free space propagation, modelled with a uniform mesh ($\Delta_x = \Delta_y = \Delta_z = \Delta_l$), the propagation constant and the characteristic impedance of the link lines are, from (3) and (4), $\gamma_{pq} = j\beta_0\Delta_l/2 = j\omega\sqrt{\mu_0\epsilon_0}\Delta_l/2$ and $Z_{pq} = Z_0 = \sqrt{\mu_0/\epsilon_0}$; (6) to (9) yield $a_{pq} = c_{pq} = 0$, $b_{pq} = d_{pq} = 1/2$, thus reducing the scattering matrix S_v to the stubless 12×12 matrix originally proposed by Johns [3]. The voltage waves at the input/output port of the link lines can be obtained by applying the following transformation:

$$\mathbf{V}_{\text{port}}^{\text{ref}} = [e^{-\gamma_{rp}\Delta_r/2}]_{\text{diag}}[S_v][e^{-\gamma_{rp}\Delta_r/2}]_{\text{diag}}\mathbf{V}_{\text{port}}^{\text{inc}} \tag{10}$$

B. Lossy Isotropic Media

If the medium to be modelled is isotropic, then the propagation constant of the link lines as given by (3) yield the same value and the characteristic impedances given by (4) vary to account for mesh grading; the matrix S_v remains as given above. The node given in [2] represents the alternate possibility where the characteristic impedance of the link lines are the same but the propagation constants vary. The node in [2] can be made to account for lossy media by replacing $\omega\sqrt{\mu\epsilon}$ with $\sqrt{(\sigma_e + j\omega\epsilon')(\sigma_m + j\omega\mu')}$ and letting the characteristic impedance of the link lines take on the complex intrinsic impedance of the medium inside the cell: $\sqrt{(\sigma_m + j\omega\mu')/(\sigma_e + j\omega\epsilon')}$.

III. Numerical Results

A. Rectangular Metallic Waveguide

Fig. 1 shows the modal dispersion characteristics of a rectangular metallic waveguide filled with a lossy dielectric. We note the excellent agreement between the analytical solution and the results computed with the FD-TLM method. The simulation of the higher-order modes is somewhat better using the frequency domain node. In particular, we note from Fig. 1(a), that the time domain nodes provide two dispersion curves for the degenerate modes TE/TM_{11} and TE/TM_{21}.

B. Shielded Rectangular Dielectric Coupler

Fig. 2 shows the shielded dielectric coupler and phase dispersion characteristics obtained using the FD-TLMmethod and the frequency domain node. Magnetic and electric walls are placed between the dielectrics in order to generate the fundamental modes having even and odd symmetry E_{11e}^y and E_{11o}^y. The results are compared to the mode-matching [11] and Fourier TLM [12] methods. Simulations using the time domain nodes were found to agree well with those obtained using the frequency domain node.

C. Computational Issues

Convergence to the analytic solutions given in Fig. 1 is quite rapid as a 10×5 mesh of TLM nodes was used to successfully generate the first seven guided modes. The results shown in Fig. 2 were obtained using a 12×8 mesh of nodes. The CPU time required per frequency point using a 10×10 mesh is about 55 minutes on a low-speed HP9000 series 400 workstation. All guided modes of interest are obtained in one sweep.

IV. Conclusion

A new frequency domain symmetrical condensed TLM node has been presented. This node is simpler to use in conjunction with frequency domain TLM techniques than time domain nodes. The performance of three TLM nodes has been compared by analysing two guiding structures. It has been

$$S_v = \left[\begin{array}{c|cccccccccccc}
 & 1 & 2 & 3 & 4 & 5 & 6 & 7 & 8 & 9 & 10 & 11 & 12 \\
1 & a_{xz} & b_{xz} & d_{xz} & & & & & & b_{xz} & & -d_{xz} & c_{xz} \\
2 & b_{xy} & a_{xy} & & & & d_{xy} & & & c_{xy} & -d_{xy} & & b_{xy} \\
3 & d_{yz} & & a_{yz} & b_{yz} & & & & b_{yz} & & & c_{yz} & -d_{yz} \\
4 & & & b_{yx} & a_{yx} & d_{yx} & & -d_{yx} & c_{yx} & & & b_{yx} & \\
5 & & & & d_{zx} & a_{zx} & b_{zx} & c_{zx} & -d_{zx} & & b_{zx} & & \\
6 & & d_{zy} & & & b_{zy} & a_{zy} & b_{zy} & & -d_{zy} & c_{zy} & & \\
7 & & & & -d_{zx} & c_{zx} & b_{zx} & a_{zx} & d_{zx} & & b_{zx} & & \\
8 & & & b_{yx} & c_{yx} & -d_{yx} & & d_{yx} & a_{yx} & & & b_{yx} & \\
9 & b_{xy} & c_{xy} & & & & -d_{xy} & & & a_{xy} & d_{xy} & & b_{xy} \\
10 & & -d_{zy} & & & b_{zy} & c_{zy} & b_{zy} & & d_{zy} & a_{zy} & & \\
11 & -d_{yz} & & c_{yz} & b_{yz} & & & & b_{yz} & & & a_{yz} & d_{yz} \\
12 & c_{xz} & b_{xz} & -d_{xz} & & & & & & b_{xz} & & d_{xz} & a_{xz}
\end{array}\right]$$

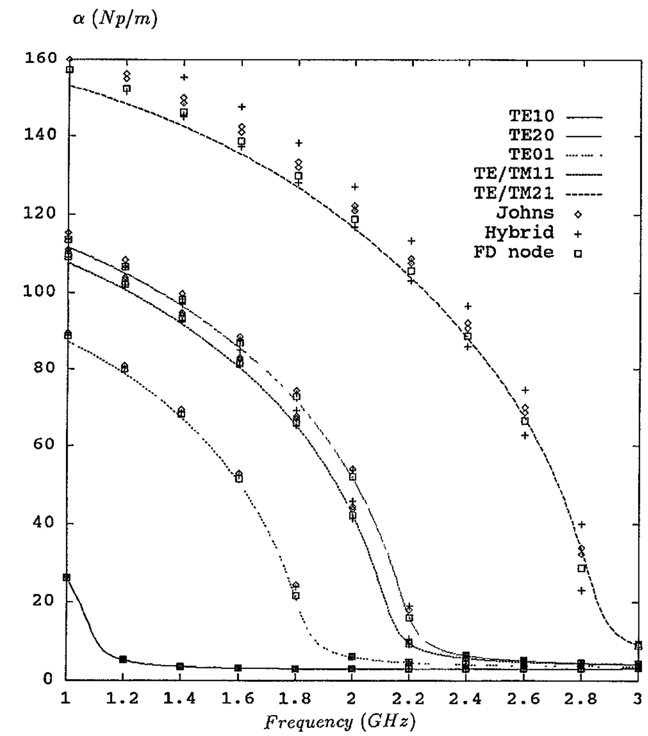

(a)

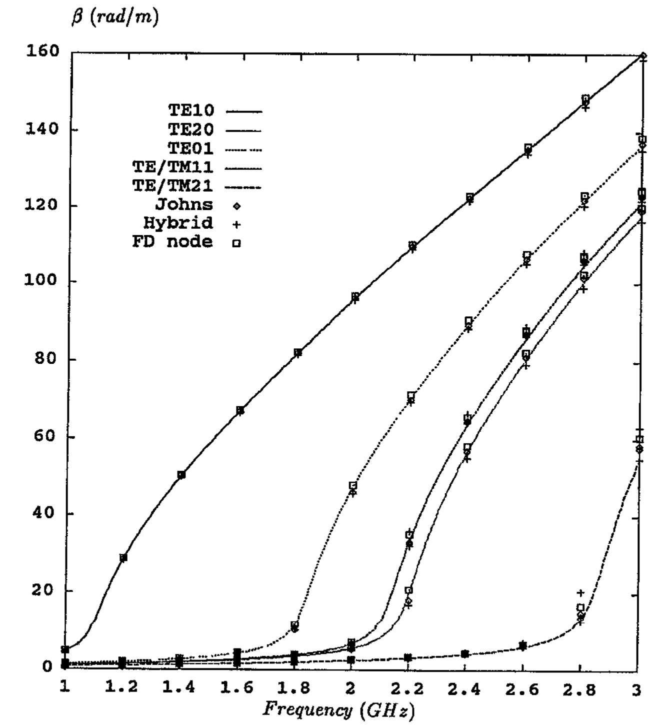

(b)

Fig. 1. Modal dispersion of a rectangular metallic waveguide filled with a lossy dielectric. (a) Attenuation constant. (b) Phase constant. Waveguide dimensions are $a = 5$ cm, $b = 3$ cm, $\epsilon_r = 3.0 - j0.04$, $\mu_r = 2.5$, and $\sigma_{se} = 0.01$ S/m.

found that all three nodes provide similar results and that they agree well with exact or published solutions.

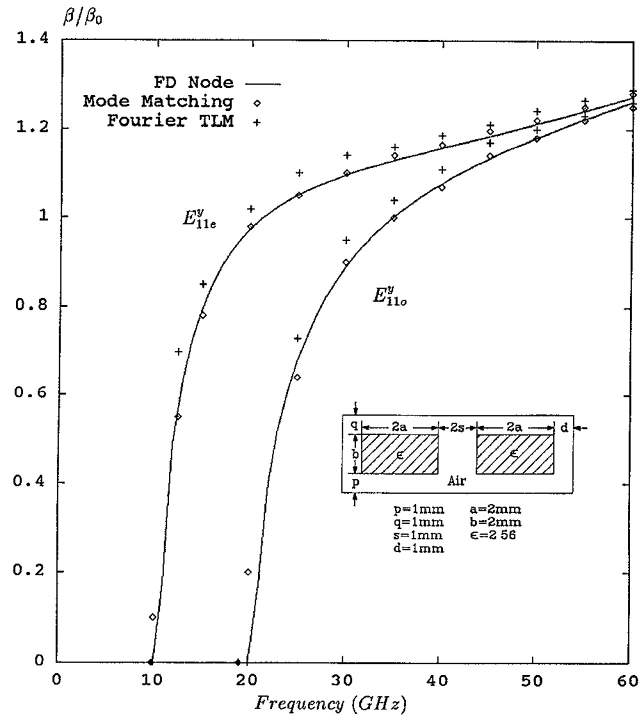

Fig. 2. Modal dispersion of a shielded dielectric coupler.

References

[1] H. Jin and R. Vahldieck, "A Frequency Domain TLM Method," *IEEE MTT-S Int. Microwave Symp. Dig.*, pp. 775–778, 1992.

[2] D. P. Johns, A. J. Wlodarczyk, A. Mallik, and C. Christopoulos, "New TLM Technique for Steady—State Field Solutions in Three Dimensions," *Electron. Lett.*, vol. 28, no. 18, pp. 1692–1694, Aug. 1992.

[3] P. B. Johns, "A Symmetrical Condensed Node for the TLM Method," *IEEE Trans. Microwave Theory Tech.*, vol. MTT-35, no. 4, pp. 370–377, Apr. 1987.

[4] P. Naylor and R. A. Desai, "New Three Dimensional Symmetrical Condensed Node For Solution of Electromagnetic Wave Problems by TLM," *Electron. Lett.*, vol. 26, no. 7, pp. 492–494, Mar. 1990.

[5] F. J. German, G. K. Gothard, and L. S. Riggs, "Modelling of Materals With Electric and Magnetic Losses With the Symmetrical Condensed TLM Method," *Electron. Lett.*, vol. 26, no. 16, pp. 1307–1308, Aug. 1990.

[6] R. Scaramuzza and A. J. Lowery, "Hybrid Symmetrical Condensed Node for the TLM Method," *Electron. Lett.*, vol. 28, no. 23, pp. 1947–1949, Nov. 1990.

[7] H. Jin and R. Vahldieck, "The Frequency-Domain Transmission Line Matrix Method—A New Concept," *IEEE Trans. Microwave Theory Tech.*, vol. MTT-40, no. 12, pp. 2207–2218, Dec. 1992.

[8] J. Huang, R. Vahldieck, and H. Jin, "Fast Frequency-Domain TLM Analysis of 3D Circuit Discontinuities," in *Proc. 9th Annual Review of Progress in Applied Computational Electromagnetics Symp.*, 1993, pp. 475–480.

[9] W. J. R. Hoefer, "The Transmission-Line Matrix Method—Theory and Applications," *IEEE Trans. Microwave Theory Tech.*, vol. MTT-33, no. 10, pp. 882–893, Oct. 1985.

[10] V. Trenkic, C. Christopoulos, and T. M. Benson, "Simple and Elegant Formulation of Scattering in TLM Nodes," *Electron. Lett.*, vol. 29, no. 18, pp. 1651–1652, Sept. 1993.

[11] A. K. Tiwari, B. Bhat, and R. P. Singh, "Generalized Coupled Dielectric Waveguide and Its Variants for Millimeter-Wave Applications," *IEEE Trans. Microwave Theory Tech.*, vol. MTT-34, no. 8, pp. 869–875, Aug. 1986.

[12] H. Jin and R. Vahldieck, "Full-Wave Analysis of Guiding Structures Using a 2-D Array of 3-D TLM Nodes." *IEEE Trans. Microwave Theory Tech.*, vol. MTT-41, no. 3, pp. 472–477, March 1993.